Environ. Sci. Technol. **2006**, *40*, 5786−5792

Ettringite-Induced Heave in Chromite Ore Processing Residue (COPR) upon Ferrous Sulfate Treatment

DIMITRIS DERMATAS,
MARIA CHRYSOCHOOU,*
DEOK HYUN MOON, DENNIS G. GRUBB,
MAHMOUD WAZNE, AND
CHRISTOS CHRISTODOULATOS

W.M. Keck Geoenvironmental Laboratory, Center for Environmental Systems, Stevens Institute of Technology, Hoboken, New Jersey 07030

A pilot-scale treatment study was implemented at a deposition site of chromite ore processing residue (COPR) in New Jersey. Ferrous sulfate heptahydrate ($FeSO_4 \cdot 7H_2O$) was employed to reduce hexavalent chromium in two dosages with three types of soil mixing equipment. XANES analyses of treated samples cured for 240 days indicated that all treatment combinations failed to meet the Cr(VI) regulatory limit of 240 mg/kg. More importantly, the discrepancy between XANES and alkaline digestion results renders the latter unreliable for regulatory purposes when applied to ferrous-treated COPR. Regardless of Cr(VI), the introduction of reductant containing sulfate, mechanical mixing, water, acidity, and the resulting temperature increase in treated COPR promoted dissolution of brownmillerite (Ca_2FeAlO_5), releasing alumina and alkalinity. The pH increase caused initially precipitated gypsum ($CaSO_4 \cdot 2H_2O$) to progressively convert to ettringite ($Ca_6Al_2(SO_4)_3 \cdot 32H_2O$) and its associated volume expansion under both in situ and ex situ conditions, with a maximum of 0.8 m vertical swell within 40 days of curing. While Cr(VI) treatment remains a challenge, the intentional exhaustion of the heave potential of COPR by transforming all Al sources to ettringite emerges as a possible solution to delayed ettringite formation, which would hamper site redevelopment.

Introduction

Chromite ore processing residue (COPR) is a byproduct of the chromite ore high-temperature lime-based roasting process that has been widely used (*1, 2*) to isolate and extract soluble chromate (CrO_4^{2-}). COPR is a granular sand-like material that was widely used as structural fill. Study Area 7 (SA7) is a 34-acre COPR deposition site located in Hudson County, New Jersey, between Route 440 and the Hackensack River that contains about 1.5 million tons of COPR, deposited between 1905 and 1954 (*3*). There are two main emerging issues with COPR: (1) residual hexavalent chromium (Cr(VI)), a known carcinogen; and (2) volumetric expansion of COPR rendering the structural fills unstable (*3*). Regulatory litigation on the environmental hazards posed by Cr(VI) has compelled the site owner to seek alternate solutions for the removal and landfill disposal of COPR (>$200 per ton). An extensive investigation was undertaken to characterize SA7 COPR and to design and implement an on-site treatment to address both the Cr(VI) hazard reduction while simultaneously mitigating the COPR heaving phenomena.

The on-site remediation of Cr(VI) involves its reduction to trivalent chromium (Cr(III)), with a target Cr(VI) concentration of 240 mg/kg (as measured by EPA methods 3060A (*4*) and 7196A (*5*)) established by the New Jersey Department of Environmental Protection (NJDEP) for residential land use (*6*). Several reductants were evaluated in a batch study, including ferrous sulfate ($FeSO_4$). While ferrous sulfate yielded satisfactory results at high stoichiometries, other studies reported its failure upon injection to COPR columns and in the field (*7, 8*). Ferrous sulfate treatment is based on the reaction

$$3Fe^{2+} + CrO_4^{\ 2-} + 8H_2O \rightarrow 4Fe_{0.75}Cr_{0.25}(OH)_3 + 4H^+ \tag{1}$$

The reason that ferrous sulfate treatment fails is that competing reactions scavenge ferrous iron (Fe(II)) before it reacts with Cr(VI), including iron oxidation

$$Fe^{2+} + \frac{1}{4}O_2(g) + \frac{5}{2}H_2O \rightarrow Fe(OH)_3 + 2H^+ \tag{2}$$

and precipitation of ferrous hydroxide or carbonate ($Fe(OH)_2$ and $FeCO_3$). Strongly alkaline conditions, such as those prevailing in COPR (pH >12) favor competing reactions. He et al. (*9*) reported that Cr(VI) reduction by Fe(II) was possible under such conditions, but higher Fe(II) dosages were necessary for complete reduction to take place, compensating for the loss of Fe(II) due to competing reactions. Moreover, the contact time and the degree of mixing between the solid phase and aqueous Fe(II) are critical in achieving early reaction between Fe(II) and Cr(VI) as they facilitate mass transfer between the solid and the liquid phases; injection does not provide adequate conditions, as previously demonstrated (*7, 8*). Accordingly, alternative methods to deliver ferrous sulfate to COPR in large quantities were sought and soil mixing (SM) techniques emerged as the most promising candidates for in situ treatment. SM technologies are routinely used in geotechnical engineering (*10*) including soil remediation applications under Superfund (*11*) and to improve marginal soils for construction and site redevelopment.

The secondary motivation to conduct a pilot study was to investigate the effect of treatment on the swell potential of COPR. In situ and ex situ soil mixing approaches modify the initial fabric of the soil/media. While this correlates to more efficient delivery of ferrous sulfate throughout COPR, it also allows for the possibility to initiate the conditions that favor ettringite ($Ca_6Al_2(SO_4)_3(OH)_{12} \cdot 26H_2O$) formation. The cementitious nature of COPR renders it a favorable candidate for ettringite formation upon sulfate influx. Ettringite is a known expansive mineral both in the cement and soil literature, and delayed ettringite formation (DEF) is one of the main mechanisms of concrete deterioration (*12*) and failure in lime-treated clays used as sub-base materials (*13, 14*). While laboratory swell tests conducted on COPR showed that ettringite formation was promoted upon sulfate addition, the role of DEF on heaving in COPR was unclear under ambient conditions (25 °C); however, swell development was unmistakable at 50 °C (*15*). The large-scale evaluation of sulfate influence of COPR was therefore an important secondary goal of the pilot study.

---

* Corresponding author tel: (201) 216 8773; fax: (201) 216 8212; e-mail: mchrysoc@stevens.edu.

10.1021/es0604461 CCC: $33.50

TABLE 1. Total Cr(VI) in Six Treatment Plots as Measured by XANES and Alkaline Digestion (AD)

	ferrous sulfate heptahydrate		total Cr (mg/kg)	Cr(VI) XANES (% of total Cr)	Cr(VI) XANES (mg/kg)	Cr(VI) AD (mg/kg)	ratio (XANES-to-AD)
	dosage	% w/w*					
HRM-5X	5×	32	16800	12.5	2100	1240	1.7
HRM-8X 8	8×	51	17600	10.5	1848	1260	1.5
VA-5X (0−2 m)	5×	38	17300	3.4	588	154	3.8
VA-5X (2−4 m)			23400	7.2	1685	460	3.7
PUG-5X	5×	32	18600	6.0	1116	384	2.9
PUG-8X	8×	51	18400	9.0	1656	421	3.9

* Percent of dry weight of untreated COPR.

Materials and Methods

Mixing Equipment. Two different types of in situ mixing equipment were used to treat the upper, unsaturated zone of SA7 COPR: a horizontal rotary mixer (HRM) and a vertical auger (VA) system (figures available in the Supporting Information). The reagent was applied in dry form to the ground surface and then mixed into the COPR using the rotating drum of the HRM. The HRM passed over the treatment area (surface area 4.5 m × 3.7 m, to depth of 1 m) twice to ensure adequate mixing. The material was then compacted to level with the original ground surface without further manipulation. The VA was a 3-m diameter double counter-rotating auger rig that was cycled up and down in the treatment zone to ensure adequate mixing. The reagent was mixed with water in the batch mixing tank of the auger to produce a slurry, which was then introduced to the COPR. Two 3-m diameter columns 4.0 m in depth (in the unsaturated zone) were completed using this equipment. Ex situ treatment featured a pugmill-type batch mixer with a 1.5 m^3 capacity (see Supporting Information), in which approximately 540 kg of moist COPR was mixed with the reagent. The pugmill was operated during the initial placement of COPR to ensure homogeneous spread in the interior of the pugmill, during the reactant addition, and further 12 min of switching the mixing direction every 2 min. The treated material was then placed into containers, and a subsample was placed in a 0.2 m^3 lined drum for long-term sampling and observations.

Reagents and Treatment Design. Ferrous sulfate heptahydrate ($FeSO_4 \cdot 7H_2O$) (Add-Iron Corporation, CAS 7782-63-0) was used at dosages calculated based on an average Cr(VI) concentration of 4000 mg/kg for the shallow HRM plots, and 4700 mg/kg for the deeper VA plots, according to eq 1. The applied dosages were 5× and 8× the stoichiometric requirement as summarized in Table 1.

Sampling. COPR samples were collected immediately prior to and following the application of the reductant, and up to 240 days curing. Fresh samples were collected from the VA and pugmill (PUG) plots at 60, 120, and 240 days, while the HRM 30-day samples were stored at ambient temperature and reanalyzed for pH and Cr(VI) at 240 days of curing. Sampling of the VA plots was performed at two depth intervals (0−2 and 2−4 m) at three locations (center of each column and midway between them). The analytical results are presented as the average of the triplicate samples by two depth intervals. Additionally, a trench was excavated in plot HRM-8X after approximately 60 days. Four horizontal layers (L1 through L4) were designated for sampling, both inside and outside (background) the treatment zone (denoted as layer-in/out).

Physicochemical Analyses. pH and water content were measured according to ASTM methods D 4980-89 and D 2216-98 (*16*), respectively. Total Cr(VI) was measured by U.S. EPA methods 3060A (*4*) and 7196A (*5*). Total metals were measured by acid digestion and inductively coupled plasma/atomic emission spectrometry (U.S. EPA methods 3015A (*17*) and 6010B (*18*)). Total sulfate was measured by an acid digestion method developed by Columbia Analytical Services (*19*).

X-ray Absorption Spectrometry. Treated samples at 240 days of curing were additionally tested for total Cr(VI) to obtain a basis for comparison with the alkaline digestion data. Samples were ground to fine powder using an agate mortar and pestle. The samples were packed to a uniform thickness and sealed with transparent adhesive tape. Cr K-edge X-ray absorption spectra (XAS) of COPR were taken on the BL7C1 (Electrochemistry) beamline in a storage ring of 2.5 GeV with a ring current of 130−185 mA (Pohang Light Source (PLS), South Korea). A complete description of the XANES analyses, data reduction, and Cr(VI) quantification method using the WinXAS software (*20*) is provided in the Supporting Information.

Mineralogical Analyses. XRPD analyses were performed on 5 samples obtained from the HRM-8X trench, 3 interior and 2 background samples at 60 days. The central sample obtained at 0−2 m below the ground surface (BGS) was analyzed from each VA plot at 120 days. Each sample (300 g) was homogenized manually and 20 g was extracted and air-dried for 24 h. Each air-dried sample was pulverized to pass a 0.4 mm sieve, homogenized again, and a 2 g subsample was selected for XRPD analysis. A McCrone micronizing mill was employed to pulverize the subsample, with cyclohexane (Fisher, CAS 110-82-7) as milling fluid, for 5 min. The slurry was air-dried for 3 h. The resulting powder was mixed with 0.2 g of α-corundum (Al_2O_3) (Sawyer, Lot C04-AO-41) on an 80/20 basis as an internal standard to quantify the amorphous phase. Step-scanned XRPD data were collected using a Rigaku DXR 3000 computer-automated diffractometer with Bragg−Brentano geometry. The diffractometry was conducted at 40 kV and 40 mA using a diffracted beam graphite-monochromator with Cu radiation. The data were collected in the range of two-theta values between 5° and 65° with a step size of 0.02° and a count time of 3 s per step. XRPD patterns were analyzed using Jade software, version 7.1 (*21*), and by reference to the patterns of the International Centre for Diffraction Data database, version 2002 (*22*), and the Inorganic Crystal Structure Database, release 2005 (*23*).

Results and Discussion

Hexavalent Chromium Treatment. Total Cr(VI) was measured by alkaline digestion (AD) in the various treatment combinations to test for regulatory compliance. Monitoring analyses were performed immediately after treatment and at various time intervals up to 240 days of curing time (Figure 1). If the AD results are to be our guide as to successful treatment, then the general trends indicated a decrease in the total Cr(VI) immediately following mixing, followed by a progressive rebound and ultimate failure by the NJDEP regulatory limit (240 mg/kg) in all plots except the VA shallow depth (0−2 m). However, the comparison of the AD data with the XANES results at 240 days (Table 1) indicates that the AD results underestimated the total Cr(VI) by a factor on the order of 1.5 to 4.0. The reasons for this discrepancy may

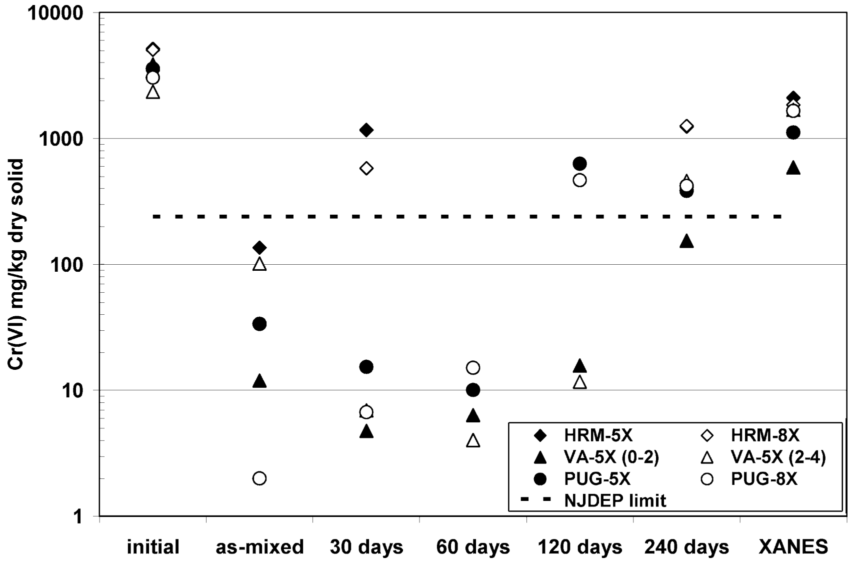

FIGURE 1. Total Cr(VI) as measured by alkaline digestion up to 240 days of treatment and as measured by XANES at 240 days curing time.

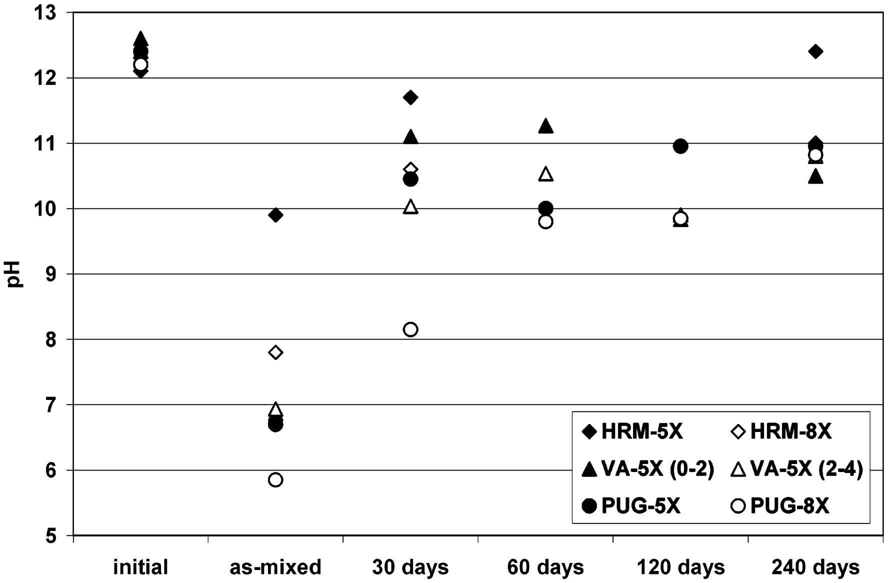

FIGURE 2. pH up to 240 days of curing time.

be that residual ferrous reduced the liberated Cr(VI) during AD and/or that Cr(VI) was not 100% released from the solid during AD. In either case, the progressive increase in the Cr(VI) concentrations measured by AD indicates that Cr(VI) did not readily dissolve from the solid matrix upon addition of ferrous sulfate, despite the apparent decrease in pH (Figure 2). Cr(VI) reduction was thus not complete at 0 day curing, contrary to AD results. Instead, Cr(VI) kept slowly diffusing out of the solid; alkaline digestion just forced a faster release during the test. If ferrous was amply available at that time, Cr(VI) was reduced during the test and yielding false positive results, as was the case at 0 day curing. With elapsed curing time and the onset of oxygen-mediated oxidation, ferrous became progressively unavailable to reduce the released Cr(VI) and the treatment appeared to have failed. Overall, the following can be concluded: (a) the AD mandated protocol is unreliable for determining Cr(VI) concentrations in COPR in the presence of Fe(II); and (b) based on XANES analyses, all treatment combinations ultimately failed the regulatory limit.

Physical and Geotechnical Properties of Treated COPR. The mixture of COPR with ferrous sulfate resembled a greenish slurry in all plots immediately following treatment. The color and texture of the HRM material changed to light-brown fine sand after 30 days, as did the pugmill samples by 120 days. The VA material remained a brown sludge up to 240 days. The changes in color and texture of the treated COPR were accompanied by pronounced volume expansion, both in the in situ plots, and all ex situ storage containers. The most pronounced heave was observed in the HRM-8X plot, estimated at 0.8 m vertical expansion by a ground survey at 40 days (see Supporting Information). Subsequent ground surveys did not show a further change in elevation in the HRM plots. The VA plots progressively presented delayed heave, reaching 0.5 m of vertical expansion at 180 days. The Supporting Information also provides images of the heaving bulge in HRM-8X, as well as images of 5-gallon polyethylene buckets that failed radially as a result of the internal swell pressures generated by the stored treated COPR. The force of the expansion was such that even the top lids of 8 oz. plastic containers were eventually torn open. The time frame for the observed expansion in the pugmill samples is not exactly known for each treatment combination; it is estimated to have stopped between 120 and 180 days. In summary, while all treatment combinations exhibited volume expansion and heave, the rate of manifestation varied significantly, with

TABLE 2. pH and Quantitative XRPD Results for Ferrous Sulfate Amended SA7 COPR Samples[a]

			background		HRM-8X (60 d)			pugmill (120 d)		VA (120 d)
			L3-out	L4-out	L2-in	L3-in	L4-in	PUG-5X	PUG-8X	VA-5X
		pH:[c]	11.4	11.5	11.1	11.6	11.6	11.0	9.8	10.4
		dilution factor:[d]	1	1	1.28	1.28	1.28	1.18	1.28	1.21
compound	**chemical formula**	**PDF**[b]								
brownmillerite	Ca_2FeAlO_5	30-0226	46.1	37.9	10.9	6.3	6.6	14.3	14.4	8.6
periclase	MgO	45-0946	2.8	2.1	1.3	0.5	1.2	1.2	1.1	0.2
brucite	$Mg(OH)_2$	07-0239	3.4	2.9	1.2	1.2	1.6	1.2	1.0	0.9
calcite	$CaCO_3$	05-0586	1.7	1.9	2.7	2.5	4.2	1.1	1.3	6.0
hydrotalcite	$Mg_6Al_2(CO_3)(OH)_{16}\cdot4H_2O$	41-1428	4.1	3.9	1.1	1.5	1.8			0.3
hydrogarnet	$Ca_3Al_2(OH)_{12}$	24-0217	9.1	10.1	2.9	3.5	5.0	4.3	2.9	2.5
ettringite	$Ca_6Al_2(SO_4)_3(OH)_{12}\cdot26H_2O$	41-1451		1.6	20.1	34.0	27.6	15.9	10.3	13.9
gypsum	$CaSO_4\cdot2H_2O$	33-0311			5.5			4.4	12.4	16.4
lepidocrocite	$FeOOH$	44-1415				2.0	3.8	1.5		
magnesiochromite	$(Mg,Fe)(Cr,Al)_2O_4$	09-0353		1.2	0.5	1.1	0.5	0.7	0.6	1.3
magnetite	Fe_3O_4	19-0629				1.4	0.9			1.1
quartz	SiO_2	46-1045			1.0	0.9	0.6			2.2
CAC[e]	$Ca_4Al_2O_6(CrO_4)\cdot14H_2O$	52-0654		0.8						
afwillite	$Ca_3(SiO_3OH)_2\cdot2H_2O$	29-0330		2.1						
amorphous			32.8	35.4	52.7	45.1	46.1	55.3	56.1	46.6

[a] All results in % w/w dry solid. [b] Powder diffraction file. [c] pH (typ). [d] Dilution factor calculated based on dry mass of added $FeSO_4$ (typ). [e] Calcium aluminum chromium oxide hydrate.

the HRM plots exhausting their heave potential within 40 days on the one end, and the VA plots continuing to swell up to 180 days on the other.

Given the fact that all in situ plots were originally compacted to ground surface, along with the observations of the COPR storage containers, it was beyond any doubt that mineralogical transformations were responsible for volumetric expansion.

pH and Mineralogical Analyses. Figure 2 shows the pH regime in the six treatment plots up to 240 days of curing. While the initial pH in untreated COPR was strongly alkaline (12.1−12.6), pH decreased in all plots immediately following mixing, to values ranging from 6 (PUG-8X) to 10 (HRM-5X) due to redox and precipitation reactions that released H^+ or consumed OH^-. H^+-releasing redox reactions include eqs 1 and 2, while OH^--consuming precipitation reactions include the formation of $Fe(OH)_2$ and $FeCO_3$. Apparently, the rate and extent of these reactions varied in the three types of mixing processes. The pH in HRM-5X dropped to 11 versus 7 in the VA-5X and PUG-5X samples. Similarly, the pH decreased to 8 in the HRM-8X plot, while the lowest pH of 6 was observed in the PUG-8X sample. The pH progressively rebounded to values exceeding 10, whereby the HRM-5X plot even attained its original pH (12.5). The observed pH rebound closely matched the Cr(VI) rebound trends (Figure 1), i.e., as the acidity originally imparted to the matrix by the addition of $FeSO_4$ was being progressively consumed, its reductive capacity was also diminished. The pH rebound was caused by ongoing mineralogical transformations in the treated COPR.

The released acidity, the decrease in pH, and the addition of high amounts of ferrous iron and sulfate caused a shift in the geochemical equilibrium of COPR and a series of mineralogical transformations. Figure 3a−c shows the XRPD pattern of untreated COPR, and PUG-8X samples at 30 days and 120 days, respectively. Table 2 shows the Rietveld quantification results for untreated (background) and select treated samples.

The mineral assemblage of untreated COPR (Figure 3a and Table 2) was consistent with COPR mineralogy reported previously (*24, 25*). Brownmillerite and periclase are the COPR parent minerals formed during the roasting process that produced COPR. These are thermodynamically unstable in aqueous environments and at ambient temperature and hydrate to form various transformation products depending on the pH and the aqueous composition. Hydrogarnet, brucite, calcium aluminum chromium oxide hydrates (CACs or monochromates), hydrotalcites, and ettringite are typical hydration products of COPR at alkaline pH (*25*). When the COPR pH decreases to values in the area of 9.5−10.5, the Al-bearing hydration products (hydrogarnet, CACs, ettringite) become unstable. Figure 3b shows that the phase $2CaO\cdot Al_2O_3\cdot8H_2O$ (or C_2AH_8 in cement nomenclature) appeared in the XRPD pattern of sample PUG-8X at pH 8; sulfate released from ferrous sulfate precipitated as gypsum, iron precipitated as goethite (FeOOH), while brownmillerite persisted; trace amounts of periclase, brucite, and calcite were also detected but are not discernible in Figure 3b. No other hydration products could be detected, which was also due to the strong preferred orientation of gypsum.

The dissolution of hydration products, and more importantly brownmillerite, progressively released alkalinity (OH^-), enabling the pH rebound. This pH shift impacted the thermodynamic equilibrium between COPR mineral phases, with the sulfate-bearing compounds (gypsum and ettringite) dominating the matrix. The gypsum−ettringite equilibrium has been extensively studied in the literature; the lower pH threshold for this transformation occurs in the range 9.5−10.5 (*26*). Furthermore, a modeling study on COPR showed that all other Al-bearing phases are metastable with respect to ettringite in the presence of sulfate (*25*). Consequently, when the pH of the treated samples increased to values above 9 (the precise value is unknown), gypsum began transforming to ettringite, thereby consuming available Al-sources, including brownmillerite. The XRPD pattern of PUG-8X (Figure 3c) confirmed the formation of ettringite at the expense of gypsum. The time evolution of other treatments indicated likewise, with Table 2 illustrating the long-term predominance of ettringite over gypsum.

Based on the observed mineralogical transformations, ettringite formation appears as the underlying mechanism to explain volume expansion in treated COPR. The needlelike structure of ettringite, its low specific gravity (G_s 1.8), and its ability to retain water render it an ideal swelling agent in cementitious systems, such as COPR. The ultimate conversion of high-density Al-bearing phases, such as brownmillerite (G_s 3.76) to ettringite, caused a large increase in volume that could not be accommodated in the existing voids of the

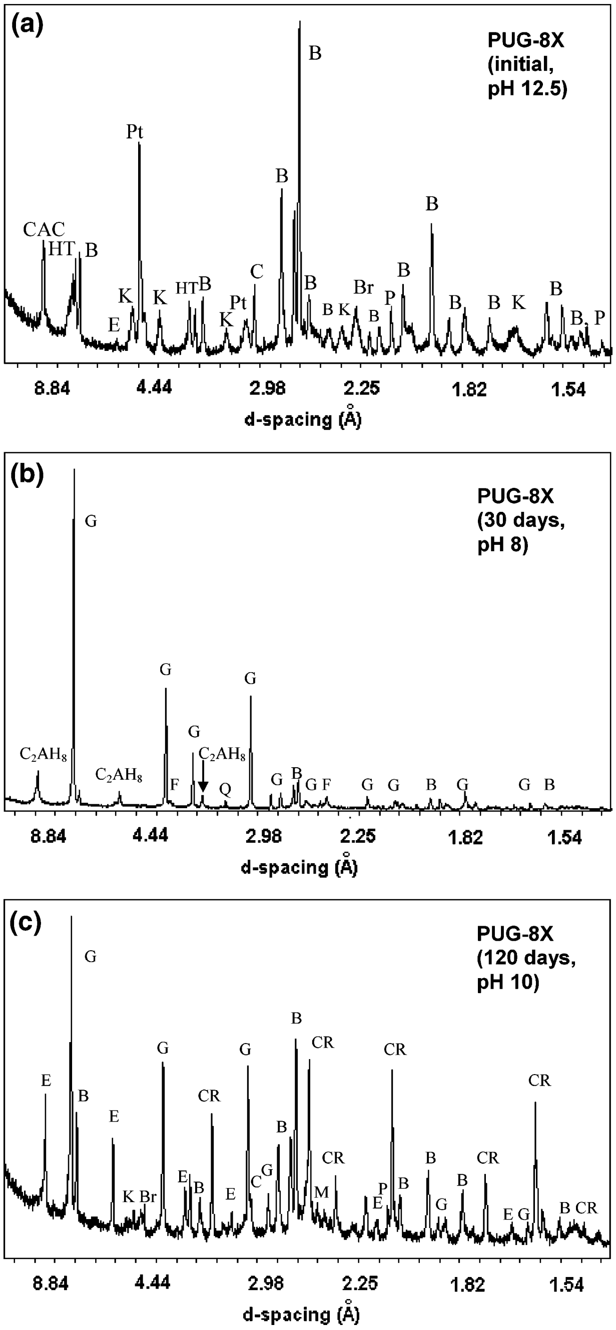

FIGURE 3. XRPD pattern of untreated COPR (a), treated pugmill 8× at 30 days curing (b), and treated pugmill 8× at 120 days curing (c). B, brownmillerite; P, periclase; K, katoite; Br, brucite; Pt, portlandite; C, calcite; E, ettringite; HT, hydrotalcite; G, gypsum; C_2AH_8, calcium alumimum oxide hydrate; F, goethite; CR, corundum; M, magnesiochromite.

compacted, treated COPR. Accordingly, the amount of the observed heave at a given point in time depended on the amount of added sulfate, the extent of transformation reactions, and the local geotechnical setting (void ratio or relative compaction, permeability, water content).

TABLE 3. Mass Balance Calculations and Total Analyses Data for Al and Sulfate in % w/w

	total sulfate (Rietveld)	total sulfate (analytical)	total Al (analytical)	stoichiometric Al for ettringite
HRM-8X	7.7	9.5	n.a.	1.8
VA-5X	12.4	15.7	n.a.	2.9
PUG-5X	6.1	5.9	4.0	1.1
PUG-8X	9.3	10.0	3.9	1.9

Table 3 demonstrates that the Rietveld-calculated and the analytical total sulfate concentrations were in very good agreement. The mass balance calculations also showed that the added sulfate was insufficient to transform the total Al to ettringite in all plots; the reaction was therefore considered complete when all gypsum was consumed to form ettringite. The XRPD quantitative results (Table 2) showed that the gypsum to ettringite transformation was complete in the deeper portions of the HRM-8X trench at 60 days. However, even though the amount of ferrous sulfate added in PUG-8X was identical to HRM-8X, transformation reactions in PUG-8X were still incomplete and the pH was lower after 120 days. Similarly, a difference in reaction rates was observed in the two plots with 5× dosage, with PUG-5X presenting a higher pH and higher degree of completion compared to the VA-5X. Overall, the HRM plots yielded the fastest reaction rate in all respects: the fastest pH rebound, the fastest dissolution of brownmillerite, and the fastest gypsum-to-ettringite conversion. The two pugmill tests presented the second fastest rebound in Cr(VI) and pH, as well as gypsum-to-ettringite conversion, but the brownmillerite dissolution rate appeared slower compared to the VA plot. However, the decrease in brownmillerite concentrations from 38−46% (background samples in Table 2) to 8−16% w/w (taking into account treatment-induced dilution) within a few weeks to months was remarkable, considering that it had remained largely unreacted in the 50−100 years of deposition at SA7. The acidity imparted through the addition of ferrous iron and associated pH decrease was a major triggering mechanism in all treatment combinations. Sulfate is also believed to have acted as a catalyst for brownmillerite hydration, as has also been observed in the literature (*27*). Additionally, temperature and water content emerged as important factors to explain the differences in reaction rates among the three treatment types.

Acid−base reactions between the released H^+ and the basic COPR minerals caused a temperature increase in the in situ plots due to cumulative release of heat. Temperatures up to 50 °C were recorded in plot VA-5X at 60 days, even in the saturated zone. The temperature regime in the HRM plots was not recorded, but anecdotal information from sampling personnel indicated elevated temperatures during the 30-day sampling event. Conversely, no change in temperature was observed in the pugmill treatments because the smaller amount of treated material and respective placement conditions allowed for the dissipation of heat. Temperature plays an important role in the rate of brownmillerite hydration (*28*). Consequently, the difference in the rates of brownmillerite hydration between the two 5× treatments (VA and PUG) and the two 8× treatments (HRM and PUG) can be attributed to the difference in the (internal) temperature regime. However, temperature does not account for the differences between the HRM-8X and VA-5X plots; the higher reductant dosage and the associated acidity would suggest a longer period of time for pH rebound and ettringite conversion in the HRM plot. Here, the role of moisture conditions is likely decisive.

The water content in the treatment plots is shown in Figure 4. The VA plot retained the highest water contents (50−60%) throughout the 240 days of monitoring. The pugmill drums were originally saturated at water content of 30%, but the water was progressively consumed to form ettringite, so that the material had a dry appearance by 120 days, even though the water content values remained the same. Furthermore, while the HRM plots appeared to maintain water content similar to that of the pugmill samples, field observations confirmed that the shallow HRM plots were subjected to

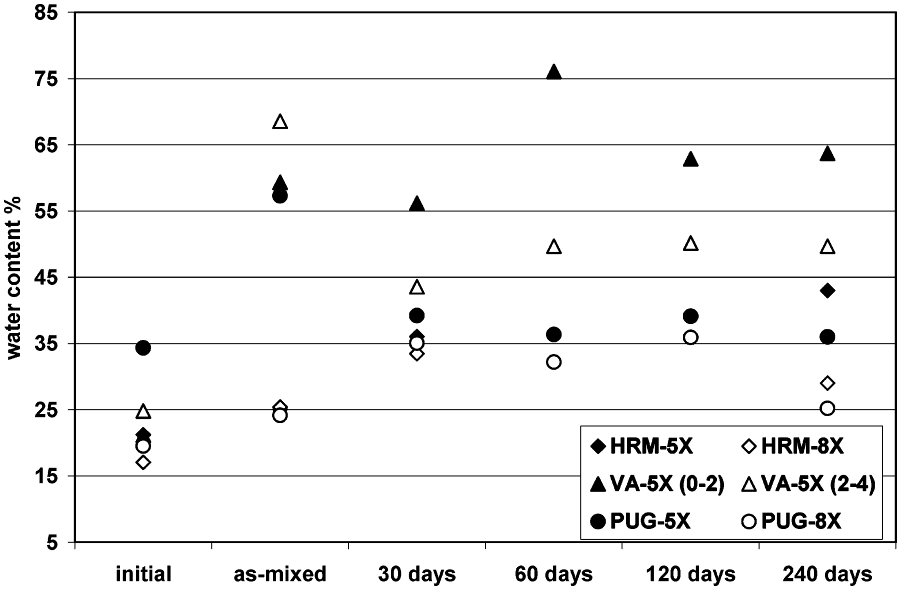

FIGURE 4. Water content up to 240 days curing time.

successive wetting and drying cycles as a result of extreme rainfall events in June 2005 (*29*). Based on these observations, it is believed that wet/dry cycles accelerate weathering reactions; similar findings were reported for steel corrosion (*30*). Conversely, the presence of ample amounts of water in the VA plot did not favor a high rate of precipitation of new phases (ettringite) and acceleration of reactions. Although an empirical observation, the water content and wet/dry cycles appear to have an important impact on reaction rates.

In summary, the influx of high amounts of sulfate in COPR, along with introduction of water, mechanical mixing, acidity, and the resulting temperature increase, led to a rapid dissolution of alumina sources (brownmillerite and its hydration products), which, in turn, resulted in significant ettringite formation and heave. This finding has important implications, not only for ferrous sulfate treatment of COPR, but also for the presence of any type of sulfate source in COPR. Most reductants used or proposed for Cr(VI) treatment in the literature (calcium polysulfide, sodium dithionite, pyrite) contain some form of sulfur that will, in part, transform to sulfate. While this transformation may never occur, or occur too slowly for ettringite-induced heave to occur, it is nevertheless a thermodynamically viable reaction favored by the alkaline pH regime that should be accounted for in treatment design. A treatability study using calcium polysulfide on COPR from Glasgow, Scotland, revealed gypsum formation in the upper layer of COPR having exposure to atmospheric oxygen (*31*). The question is, can one tolerate the risk to develop heave if ettringite forms under favorable pH conditions and in adequate amounts? While this may never happen, it is a question of financial risk when the redevelopment of sites with high commercial value, such as SA7, is concerned. The geotechnical properties of the treated material are equally important with the success of the reductive treatment, whether the material remains in place or moved to a landfill. This speaks for four potential management strategies:

1. Ettringite-induced heave may be eliminated by permanently decreasing the pH below the ettringite stability domain. The extremely high alkalinity of COPR renders this approach financially and practically unfavorable.

2. Non-sulfur based treatments may be considered. For example, the addition of barium hydroxide has the potential to immobilize both chromate and sulfate and resolve both issues associated with COPR: Cr(VI) contamination and heaving (*25*).

3. The oxidation of sulfur from sulfide-based reactants may be eliminated by isolating the treated material from the atmosphere and/or using an additional oxygen-scavenger.

4. The heaving potential of COPR can be intentionally exhausted by transforming all available alumina sources to ettringite. For example, waste gypsum could be used in conjunction with ferrous sulfate to transform all Al-bearing minerals to ettringite. The most important consideration in this approach is the time it takes for complete transformation, COPR recompaction, and site redevelopment. The SA7 pilot study demonstrated that the implementation method significantly affects reaction rates. This solution also requires a detailed study of the geotechnical properties of the resulting ettringite matrix to ensure that these are adequate for site redevelopment.

Acknowledgments

We thank Honeywell International Inc. for the financial support of the COPR investigation; Geosyntec Consultants for the execution of the pilot scale study and for providing the images of the equipment and the ground survey data; and Dr. Richard Magee for his input in the treatment design and evaluation. We are also grateful to the authorities at the Pohang Light Source (PLS) and Dr. Min Gyu Kim for the XANES data collection.

Supporting Information Available

Detailed description of the Cr(VI) quantification procedure, supplemental figures of equipment used in the pilot testing, XANES spectra, and photos of the heaved plots and failed buckets of treated COPR. This material is available free of charge via the Internet at http://pubs.acs.org.

Literature Cited

(1) McKee, T. *Chromate Chemical Production Industry: Waste Treatment Past and Present*; Report to the New Jersey Department of Environmental Protection: Trenton, NJ, 1988.

(2) Darrie, R. G. Commercial extraction technology and process waste disposal in the manufacture of chromium chemicals from ore. *Environ. Geochem. Health* **2001**, *23*, 187−193.

(3) Dermatas, D.; Bonaparte, R.; Chrysochou, M.; Moon, D. H. Chromite Ore Processing Residue (COPR): Hazardous contaminated soil or solid waste? *J. ASTM Int.* **2006**, *3* (*7*).

(4) U.S. Environmental Protection Agency. *Alkaline Digestion for Hexavalent Chromium, Method 3060A*; USEPA: Washington, DC, 1996.

(5) U.S. Environmental Protection Agency. *Chromium, Hexavalent (colorimetric), Method 7196A*; USEPA: Washington, DC, 1992.
(6) New Jersey Department of Environmental Protection. *Summary of the basis and background of the soil cleanup criteria for trivalent and hexavalent chromium*; NJDEP: Trenton, NJ, 1998.
(7) Geelhoed, J. S.; Meussen, J. C. L.; Roe, M. J.; Hillier, S.; Thomas, R. P.; Farmer, J. G.; Paterson, E. Chromium remediation or release? Effect of iron(II) sulfate addition on chromium(VI) leaching from columns of chromite ore processing residue. *Environ. Sci. Technol.* **2003**, *37*, 3206−3213.
(8) Su, C.; Ludwig, R. D. Treatment of hexavalent chromium in chromite ore processing solid waste using a mixed reductant solution of ferrous sulfate and sodium dithionite. *Environ. Sci. Technol.* **2005**, *39*, 6208−6216.
(9) He, Y. T.; Chen, C.; Traina, S. J. Inhibited Cr(VI) reduction by aqueous Fe(II) under hyperalkaline conditions. *Environ. Sci. Technol.* **2004**, *38*, 5535−5539.
(10) Bruce, D. A. The return of deep soil mixing. *Civil Eng.* **1996**, *66* (*12*), 44−46.
(11) U.S. Environmental Protection Agency. *International waste technologies/ Geo-Con in-situ stabilization/solidification*; Application Analysis Report, EPA/540/A5-89/004; USEPA: Washington, DC, 1990.
(12) Taylor, H. F. W.; Famy, C.; Scrivener, K. L. Review Delayed Ettringite Formation. *Cem. Concr. Res.* **2001**, *31*, 683−693.
(13) Mitchell, J. K. Practical problems from surprising soil behavior. *J. Geotech. Eng.* **1984**, *112* (*3*), 250−289
(14) Dermatas, D. Ettringite-induced heaving in soils: State-of-the-art. *Appl. Mech. Rev.* **1995**, *38* (*10*), 659−673.
(15) Moon, D. H.; Dermatas, D.; Chrysochoou, M.; Sanchez, A.; Grubb, D. G. *Sulfate-induced heaving in Chromite Ore Processing Residue*; 5th Conference on Environmental Geotechnics Proceedings, 26−30th June, Cardiff, United Kingdom, 2006.
(16) American Society for Testing and Materials. *Annual Book of ASTM Standards, Soil and Rock*; ASTM: West Conshohocken, PA, 2005; Vol. 4.08.
(17) U.S. Environmental Protection Agency. Microwave assisted acid digestion of aqueous samples and extracts; SW-846, Method 3015A; USEPA: Washington, DC, 1998.
(18) U.S. Environmental Protection Agency. Inductively Coupled Plasma − Atomic Emission Spectrometry, Method 6010B; USEPA: Washington, DC, 1996.
(19) Columbia Analytical Services. *Acid Digestion for Sulfate*; Kelso, WA, 2005.
(20) Ressler, T. WinXAS: a program for X-ray absorption spectroscopy data analysis under MS−Windows. *J. Synchrotron Radiat.* **1998**, *5*, 118−122.
(21) Material's Data Inc. *Jade, Version 7.1*; 2005.
(22) International Centre for Diffraction Data. *Powder Diffraction File PDF-2 Database Release*; ICDD: Newtown Square, PA, 2002.
(23) Inorganic Crystal Structure Database. Fachinformationszentrum Karlsruhe, Germany, 2005.
(24) Hillier, S.; Roe, M. J.; Geelhoed, J. S.; Fraser, A. R.; Farmer, J. G.; Paterson, E. Role of quantitative mineralogical analysis in the investigation of sites contaminated by chromite ore processing residues. *Sci. Total Environ.* **2003**, *308*, 195−210.
(25) Chrysochoou, M.; Dermatas, D.; Moon, D. H.; Christodoulatos, C.; Wazne, M.; French, C.; Morris, J.; Kaouris, M. Investigation of barium treatment of Chromite Ore Processing Residue *J. ASTM Int.* **2006**, *3* (*6*).
(26) Chrysochoou, M.; Dermatas, D. Evaluation of ettringite and hydrocalumite formation for heave metal immobilization: Literature review and experimental study *J. Haz. Mater.* **2006**, *136*, 20−33.
(27) Meller, N.; Hall, C.; Jupe, A. C.; Colston, S. L.; Jacques, S. D. M.; Barnes, P.; Phipps, J. The paste hydration of brownmillerite with and without gypsum: a time-resolved synchrotron diffraction study at 30, 70, 100 and 150 °C. *J. Mater. Chem.* **2001**, *14*, 428−435.
(28) Jupe, A. C.; Cockcroft, J. K.; Barnes, P.; Colston, S. L.; Sankar, G.; Hall, C. The site occupancy of Mg in brownmillerite structure and its effect on hydration properties: an X-ray/neutron diffraction and EXAFS study *J. Appl. Crystallogr.* **2001**, *34*, 55−61.
(29) Office of the New Jersey State Climatologist. Homepage. ONJSC at Rutgers University: Piscataway, NJ. http://climate.rutgers.edu/stateclim.
(30) Yamashita, M.; Konishi, H.; Kozakura, T.; Mizuki, J.; Uchida, H. In situ observation of initial rust formation process on carbon steel under Na_2SO_4 and NaCl solution films with wet-dry cycles using synchrotron radiation X-rays. *Corros. Sci.* **2005**, *47*, 2492−2498.
(31) Graham, M. C.; Farmer, J. G.; Anderson, P.; Paterson, E.; Hillier, S.; Lumsdon, D. G.; Bewley, R. J. F. Calcium polysulfide remediation of hexavalent chromium contamination from chromite ore processing residue. *Sci. Total Environ.* **2006**, *364*, 32−44.

Received for review February 24, 2006. Revised manuscript received June 26, 2006. Accepted June 28, 2006.

ES0604461